International Journal of Environmental Sciences
ISSN: 2229-7359
Vol. 11 No. 8, 2025
https://www.theaspd.com/ijes.php

Application Of The FAO-56 Approach To Calculate Evapotranspiration By Using Remote Sensing Data

Djellouli Riad[a*] and Bachir Bouiadjra Salah Eddine,[a] and González-Méndez Blanca [b,c]
[a]Laboratiore de Valorisation des phyto-ressources et écodéveloppement des espaces, Djilali Liabes University, Sidi Bel Abbes, Algérie ; [b]CONACYT, Benito Juárez, Mexico City, Mexico ; [c] Estación Regional del Noroeste, Colosio y Madrid s/n, Universidad Nacional Autónoma de México, Hermosillo Sonora, Mexico.
Djilali Liabes University, Laboratoire de Valorisation des phyto-ressources et écodéveloppement des espaces, route de Tlemcen, Sidi Bel Abbes, Algérie, 22000, *E-mail : djellouli_riad@yahoo.fr riad.djellouli@univ-sba.dz

Abstract: *The growing demand of water resources around the world caused by global drought have severely reduced agricultural yield in semi-arid regions. So, to tackle this issue, remote sensing data can be utilized to determine the water needs of crops by assessing the crop coefficient (K_c) and actual evapotranspiration (ET_c). This research presents a methodology for determining K_c and reference evapotranspiration (ET_0) utilizing the FAO-56 method. Images of Landsat 8 satellite and meteorological data were employed to calculate ET_c, with ET_0 obtained via the Penman-Monteith equation. Additionally, vegetation indices, including the normalized difference vegetation index (NDVI) and the soil-adjusted vegetation index (SAVI). The results demonstrate a strong correlation between predicted and observed K_c values, validating the methodology's accuracy. The technique has considerable efficacy in high-resolution satellite imaging and signifies a crucial advancement in precision agriculture for arid and semi-arid areas.*
Keywords: *FAO-56, Landsat 8, crop coefficient, actual evapotranspiration.*

INTRODUCTION:

Algeria is one of the many countries in the world facing water shortages. This can be attributed to a persistent drought and an increased demand for water in various sectors, particularly irrigation. Consequently, water deficit and hydric stress significantly affect grain yield [1]. In addition, reduced irrigation and an edaphic drought also affect the growth and height of the plant [2].

Several techniques have been adopted to estimate the water deficit. The most commonly used technique, referred to as the FAO-56 dual crop coefficient approach [3], makes use of the reference evapotranspiration ET_0 and the crop coefficient k_c. The coefficient estimates plant transpiration and soil evaporation, based on the density of the vegetation cover [4].

Furthermore, the growth and development of plants is widely restrained by the low soil moisture levels and water irrigation scarcity[5]. this requires the development of effective methods to be able to manage the resource rationally. To tackle these pressing issues, a variety of methods have been developed to assess water deficits[6], among which the FAO-56 crop coefficient method is a significant and commonly employed technique [7].

Remote sensing data have been used to study water deficits by estimating parameters related to the phenological stages of plants[8]. The crop coefficient can be indirectly estimated by analysing the reflectance of objects through remote sensing [9]. This makes it possible to spatiotemporally monitor k_c and the crop evapotranspiration ET_c by using vegetation indices [10], including the normalized difference vegetation index (NDVI) and the soil adjusted vegetation index (SAVI), These two indices contribute to predicting the crop coefficient at a regional level [11]. This has enabled multiple researchers to explore the relationship between seasonal variations, vegetation indicators, and evapotranspiration.

Study Area:

The plain of Sidi Bel Abbes, located in northwest Algeria, was analysed in the current study. The primary reason behind conducting this study on 7 hectares of the plain of Sidi Bel Abbes is its vast cereal fields, as shown in Fig. 1. The soil is of the sandy loam type, and the region has a semi-arid Mediterranean climate with an average annual rainfall and temperature of 442 mm and 15.7 °C, respectively [12].

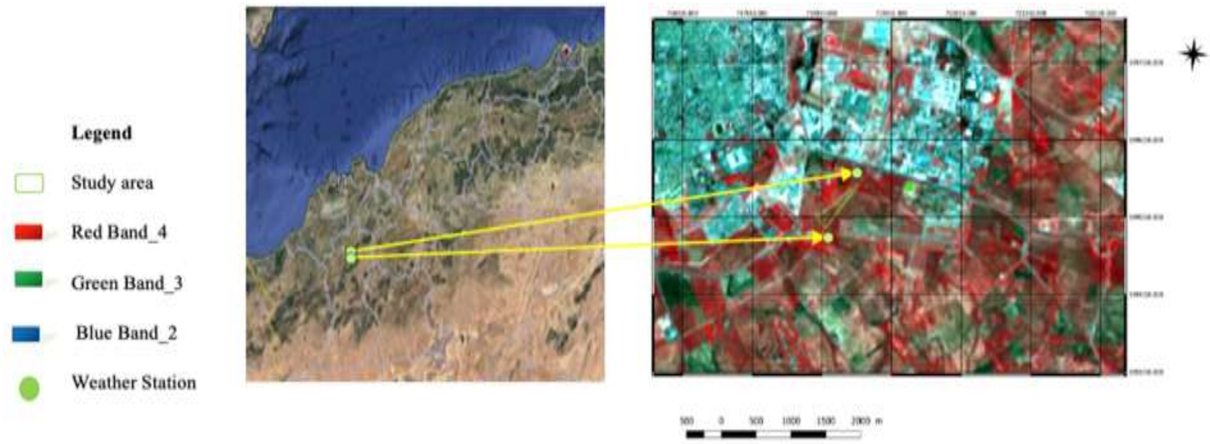

Fig. 1 False colour composition images of the study area obtained by Landsat 8 satellite (5, 4, 3).

Methodology:

Wheat was sown towards the end of November 2017 and harvested in June 2018. We calculated the crop coefficient K_c by measuring the average height of 20 different wheat plant samples, as shown in Eq. 3. The meteorological station of Sidi Bel Abbes city (35°17' N 0° 60 W) provided the climatic data. We estimated the crop coefficient K_c based on the values of NDVI and SAVI obtained from images captured by the Landsat 8 satellite.

The wheat plant samples were collected after the following time intervals:

- After the first stage of growth, i.e., 60 days after planting.
- After the second stage of growth, i.e., 90 days after planting.
- After the ripening stage, i.e., 180 days after planting.

The Penman-Monteith equation was employed to calculate the reference evapotranspiration (ET_0), as illustrated in Eq. 1.

$$ET_0 = \frac{0.408\Delta(R_n - G) + \gamma\left(\frac{900}{T + 273}\right)u_2(e_s - e_a)}{\Delta + \gamma(1 + 0.34u_2)} \qquad (1)$$

Where

- ET_0: refer to the reference evapotranspiration [mm day^{-1}].
- Rn: net radiation from the crop surface [MJ m day^{-1}].
- G: soil heat flux density [MJ m^{-2} day^{-1}].
- T: mean daily air temperature at an elevation of 2 m [^{0}C],
- u2: wind speed at an elevation of 2 m [m s^{-1}],
- e_s: saturation vapor pressure [kP_a].
- e_a: actual vapor pressure [kP_a].
- (e_s–e_a): the saturation vapor pressure deficit [kP_a].
- Δ: slope vapor pressure curve [kP_a $^0C^{-1}$].

The actual evapotranspiration ET_c is given as

$$ETc = ET0 \times Kc \qquad (2)$$

The crop coefficient depends on the phenological stage and the duration of the growth stages of the plant [13]. The k_c coefficients at different stages have been adapted to the field data by using Eq. 3 [14].

$$k_{cStage(n)} = k_{c\,Stage(n)(Tab)} + [(0.04(u_2 - 2) - 0.004(RH_{min} - 45)]\left(\frac{h}{3}\right)^{0.3} \qquad (3)$$

Where K_c Stage (n) (Tab), RHmin, and h refer to the standard coefficient value obtained from the FAO-56 approach [15], minimal relative moisture value for each day during the growth stages [%], and height of the plant for each growth stage [m] (0.1 <h<10 m), respectively.

The NDVI index was calculated from the images of the three growth stages obtained from the Landsat 8 satellite, as shown in Eq. 4.

$$\mathrm{NDVI} = \frac{\rho_{NIR} - \rho_{red}}{\rho_{NIR} + \rho_{red}}, \tag{4}$$

Where ρ_{NIR} and ρ_{red} represent the reflectance of the near-infrared and red bands, respectively. NDVI was used because chlorophyll absorbs the red band of the incoming sunlight and the spongy mesophyll structure of the leaves reflects high proportions of the incident near-infrared band (NIR) [16].

The Soil-Adjusted Vegetation Index (SAVI) was developed from the images of the three growth stages collected from the Landsat 8 satellite, as illustrated in Eq. 5.

$$\mathrm{SAVI} = (1 + L) * \frac{\rho_{NIR} - \rho_{red}}{\rho_{NIR} + \rho_{red} + L} \tag{5}$$

L is a parameter that minimizes the influence of the ground and varies from 0 to 1.

Results and Discussion: The reference evapotranspiration was calculated by using the ET_0 1.0 software. The minimum and maximum values of ET_0 were recorded in December and May, respectively. The values of ET_0, relative humidity, wind speed, and maximum and minimum temperatures are shown in Table 1. The rise in temperature and drop in relative humidity during the study period increased the loss of water from the soil-plant system to the atmosphere.

Table 1 The meteorological measurements for the growth phases 2017-2018.

Month	**Min Temperature ^{O}C**	**Max temperature ^{O}C**	**Relative humidity (%)**	**Wind speed (m/s)**	**ET_0 (mm day^{-1})**
November	2.5	28.9	65	3.4	4.1
December	-2.2	20.4	82	2.3	1.8
January	-3.3	20.1	77	3.7	2.5
February	-2.4	24.3	69	4.3	4.1
March	0.7	28.4	60	3.3	5.1
April	0.4	29.5	52	3.2	5
May	5.3	35.4	51	3.7	8.6

The Normalized Difference Vegetation Index (NDVI) and Soil-Adjusted Vegetation Index (SAVI) show a significant increase during the second growth stage, which corresponds to the active growth phase of vegetation marked by increased chlorophyll activity [17]. As the crop advances to the third stage, known as maturity, and temperatures increase, both NDVI and SAVI values decline Figures 2 and 3 indicate the reduction in chlorophyll activity [18].

(a) (b) (c)

Fig. 2 Normalized difference vegetation index (NDVI) for the (a) first, (b) second, and (c) third growth stages.

(a) (b) (c)

Fig. 3 Soil-adjusted vegetation index (SAVI) for the (a) first, (b) second, and (c) third growth stages.

The linear regression equations of K_c at different stages of growth are calculated and shown in Table 2. The correlation coefficient R^2 between the vegetation indices (NDVI and SAVI) was equal to 0.93, 0.87, and 0.87 for the first, second, and third stages of growth, respectively. The values of R^2 and R^2 adjusted during the three growth stages, were significant because the coefficients are close to each other, which explains that there is a strong linear relationship between K_c and NDVI SAVI[18], and the minimal RMSE values confirm that the model fits the data, which further confirms the significance of this model concerning the data used.

The results obtained in the current study are similar to the ones obtained in a similar survey conducted in a semi-arid climate by using images from the SPOT-4 and Landsat satellites [19].

Table 2 The predictive equations of various coefficients for stages of development.

Growth stage	Prediction equation	R^2	Adj R^2	RMSE
First growth stage	K_c = -0.613+(0.4*NDVI) +(1.7*SAVI)	0.93	0.91	0.0013
Second growth stage	K_c=0.794+(0.103*NDVI) +(0.408*SAVI)	0.87	0.84	0.0095
Third growth stage	K_c = 0.286+(2.96*NDVI) +(-1.64*SAVI)	0.87	0.81	0.0097

Table 2 presents the predictive equations for crop coefficients K_c across three growth stages, utilizing NDVI (Normalized Difference Vegetation Index) and SAVI (Soil-Adjusted Vegetation Index) as predictors. The table includes key statistical parameters, namely R^2, adjusted R^2 (Adj R^2), and RMSE (Root Mean Square Error), which assess the equation's performance. For the first growth stage, the equation explains 93% of the variance in K_c (R^2 = 0.93, Adj R^2 = 0.91), with a minimal RMSE of 0.0013, indicating high predictive accuracy. During the second development stage, the equation explains for 87% of the variation in K_c (R^2 = 0.87, Adj R^2 = 0.84) with an (RMSE) of 0.0095. This indicates a moderate predictive accuracy, comparing it to the first growth stage.

The equation for the third growth stage exhibits a similar R^2 (0.87) to R^2 (0.87) of second growth stage but a diminished adjusted R^2 (0.81) and a higher RMSE (0.0097), indicating that this model's accuracy is comparatively lower to the others. Overall, the table highlights the efficacy of NDVI and SAVI as predictors, particularly in the early growth stage, where predictive accuracy is optimal.

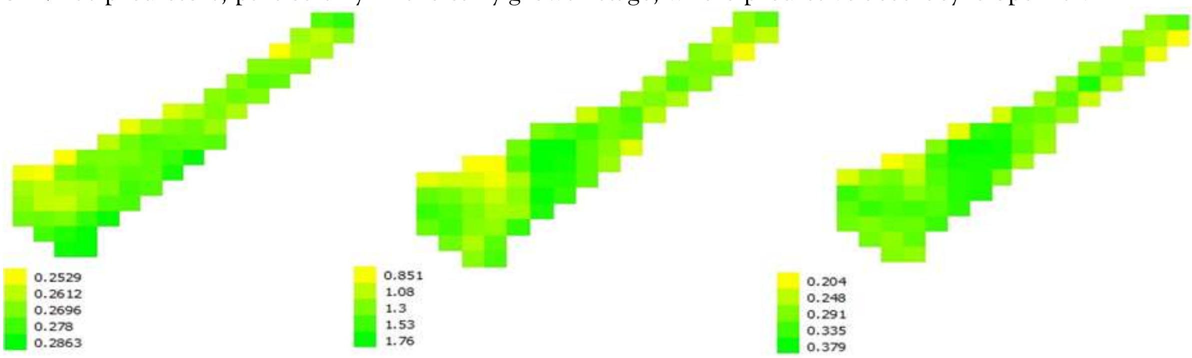

(a) (b) (c)

Fig. 4 Predicted crop coefficient K_c for the (a) first, (b) second, and (c) third growth stages.

In Fig.4 after modelling the K_c coefficient by NDVI and SAVI by a linear model, this parameter was spatialized to convert it to a map, to know its value corresponding to the terrain, to calculate the evapotranspiration at the pixel scale.
The actual evapotranspiration of wheat crop was calculated by multiplying K_c with ET_0, as shown in Fig. 5.

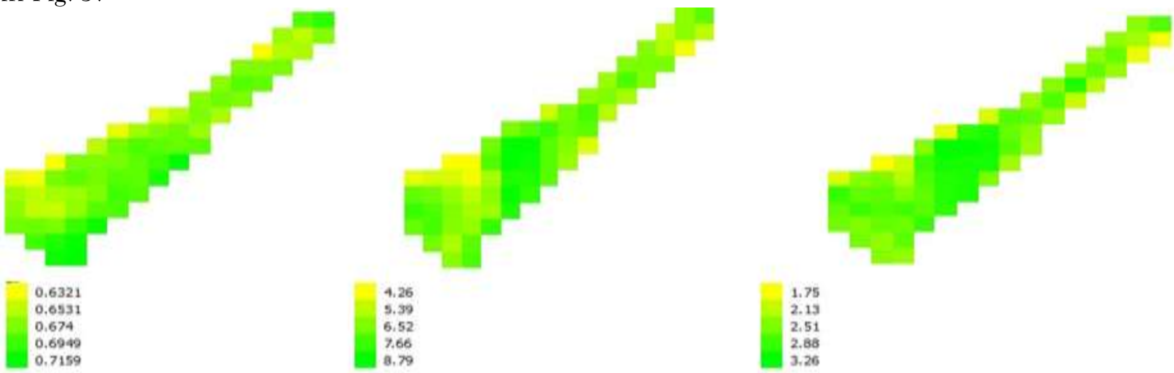

(a) (b) (c)
Fig. 5 Predicted crop evapotranspiration ET_c for the (a) first, (b) second, and (c) third growth stages.

The NDVI, SAVI, K_c, and predicted K_c parameters demonstrate similar variation trends across different stages of growth, as shown in Fig. 6.

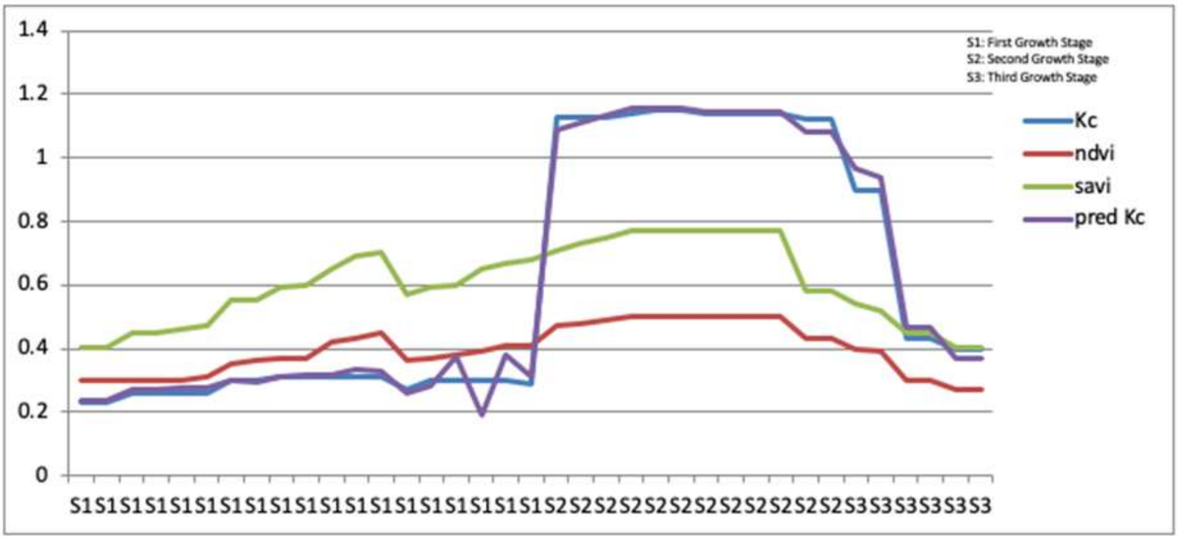

Fig. 6 Variation of Kc, NDVI, SAVI, and predicted Kc across different growth stages.

Figure 6 shows the variation of the field and predicted K_c, NDVI, and SAVI across different growth stages. It is noteworthy that the maximum values of these indices are recorded during the second growth stage. This indicates that the crop evapotranspiration was maximum during the second growth stage [20]. Similar observations were reported by [21] and [20].
Detailed statistical analyses have shown that the correlation coefficient R^2 between the estimated and predicted crop coefficient K_c is equal to 0.93, 0.98, and 0.98 for the first, second, and third stages of growth, respectively, as shown in Table 3. This confirms the accuracy of the proposed technique in calculating the actual evapotranspiration.

Table 3 Correlation coefficients for different growth stages between the values of calculated and predicted K_c.

Growth stage	Correlation	Signif. Prob.
First-season growth stage	0.93	0.00001*

Second-season growth stage	0.98	0.00001*
Third-season growth stage	0.98	0.00001*

However, it is important to note that estimating crop water requirements by using images from the Landsat 8 satellite is satisfactory as long as the fraction of water evaporated from the soil is neglected, and the vegetation is not stressed [22].
The FAO-56 approach has demonstrated efficacy in estimating evapotranspiration worldwide, especially in arid and semi-arid regions [23]. The resolution of the images used in the present study (30 m) [24], as well as that of the images used by [21] (20 m), is sufficient and can compensate for the lack of data on parameters like the spatial data, because there are regions in the world that are not well covered by satellite images [25].

CONCLUSION: The current study discusses the application of the FAO-56 coefficient approach in measuring evapotranspiration by using remote sensing. Images from the Landsat 8 satellite were used to model K_c and subsequently calculate the actual evapotranspiration. The correlation coefficients R^2 between the vegetation indices were equal to 0.93, 0.87, and 0.87 for the first, second, and third stages of growth, respectively. Similarly, the adjusted correlation coefficients adj R^2 between the vegetation indices were equal to 0.91, 0.84, and 0.81 for the first, second, and third stages of growth, respectively.
It was found that the values of evapotranspiration obtained by remote sensing were satisfactory if water stress and evaporation from the soil were neglected. The maximum water requirements were observed during the second growth stage. However, it is important to ensure that the spatial resolution of the images used for implementing the FAO-56 coefficient approach is sufficient to compensate for the lack of data on parameters like the spatial cultural coefficient.
The findings of this study highlight the robustness of the FAO-56 coefficient approach in estimating evapotranspiration using remote sensing, paving the way for its broader application in precision agriculture, water resource management, and climate modeling. Future research could focus on integrating high-resolution satellite imagery and advanced machine learning algorithms to further refine the accuracy of K_c modeling and evapotranspiration estimation, particularly in regions with complex topography or heterogeneous vegetation. Additionally, incorporating parameters such as soil moisture content, water stress indices, and localized cultural coefficients into the model can enhance its predictive capabilities. The study's methodology holds significant potential for optimizing irrigation practices and addressing water scarcity challenges, making it highly relevant in the context of sustainable agriculture and environmental conservation.
Acknowledgements, Thanks to all the people and organizations that helped make this study possible, the writers feel great about finishing it. Many thanks to those who helped with technical issues and gave access to remote sensing data that made it possible to look at how much water crops need in semi-arid areas. At the same time, we want to thank our colleagues who helped shape this study by sharing their ideas and giving us feedback. Their knowledge was very helpful in improving the method and making the results more accurate. Lastly, we want to thank everyone who has worked to promote sustainable water management methods, which are in line with the study's goals. Without the help and cooperation of these people, this work would not have been possible.

REFERENCES:
[1] S. K. Sandal et C. L. Acharya, « Effect of conservation tillage on moisture conservation, soil-physical conditions, seedling emergence and grain yield of rainfed maize (Zea mays) and wheat (Triticum aestivum) », *The Indian Journal of Agricultural Sciences*, vol. 67, nº 6, Art. nº 6, 1997, Consulté le: 28 janvier 2025. [En ligne]. Disponible sur: https://epubs.icar.org.in/index.php/IJAgS/article/view/29896
[2] J. P. Lynch, « Edaphic stress interactions: Important yet poorly understood drivers of plant production in future climates », *Field Crops Research*, vol. 283, p. 108547, juill. 2022, doi: 10.1016/j.fcr.2022.108547.
[3] L.-E. Olivera-Guerra *et al.*, « Modeling actual water use under different irrigation regimes at district scale: Application to the FAO-56 dual crop coefficient method », *Agricultural Water Management*, vol. 278, p. 108119, mars 2023, doi: 10.1016/j.agwat.2022.108119.

[4] D. W. Mebrie, T. T. Assefa, A. Y. Yimam, et S. A. Belay, « A remote sensing approach to estimate variable crop coefficient and evapotranspiration for improved water productivity in the Ethiopian highlands », *Appl Water Sci*, vol. 13, nº 8, p. 168, juill. 2023, doi: 10.1007/s13201-023-01968-5.
[5] S. Kumar, S. Shivani, S. Mishra, et V. P. Singh, « Effect of tillage and irrigation on soil-water-plant relationship and productivity of winter maize (Zea mays) in north Bihar », *The Indian Journal of Agricultural Sciences*, vol. 76, nº 9, Art. nº 9, 2006, Consulté le: 29 janvier 2025. [En ligne]. Disponible sur: https://epubs.icar.org.in/index.php/IJAgS/article/view/3061
[6] S. Ma, S. Liu, Z. Gao, X. Wang, S. Ma, et S. Wang, « Water Deficit Diagnosis of Winter Wheat Based on Thermal Infrared Imaging », *Plants*, vol. 13, nº 3, Art. nº 3, janv. 2024, doi: 10.3390/plants13030361.
[7] C. Fu *et al.*, « Combining the FAO-56 method and the complementary principle to partition the evapotranspiration of typical plantations and grasslands in the Chinese Loess Plateau », *Agricultural Water Management*, vol. 295, p. 108734, avr. 2024, doi: 10.1016/j.agwat.2024.108734.
[8] P. Karmakar, S. W. Teng, M. Murshed, S. Pang, Y. Li, et H. Lin, « Crop monitoring by multimodal remote sensing: A review », *Remote Sensing Applications: Society and Environment*, vol. 33, p. 101093, janv. 2024, doi: 10.1016/j.rsase.2023.101093.
[9] N. Pampaniya *et al.*, « Estimation of Crop Coefficients Using Landsat-8 Remote Sensing Image at Field Scale for Maize Crop », in *Geospatial Practices in Natural Resources Management*, P. K. Shit, D. Dutta, T. K. Das, S. Das, G. S. Bhunia, P. Das, et S. Sahoo, Éd., Cham: Springer International Publishing, 2024, p. 463-477. doi: 10.1007/978-3-031-38004-4_21.
[10] A. Nagy *et al.*, « Precision Estimation of Crop Coefficient for Maize Cultivation Using High-Resolution Satellite Imagery to Enhance Evapotranspiration Assessment in Agriculture », *Plants*, vol. 13, nº 9, Art. nº 9, janv. 2024, doi: 10.3390/plants13091212.
[11] M. Singh, A. R. Pimpale, M. M. Deshmukh, P. B. Rajankar, et I. K. Ramteke, « Estimation of Wheat Crop Coefficient Using GIS and Remote Sensing- A Case Study of Akola District of Maharashtra, India », *J. Sci. Res. Rep.*, vol. 30, nº 9, p. 41-50, août 2024, doi: 10.9734/jsrr/2024/v30i92328.
[12] I. Mahcer, D. Baahmed, L. Oudin, et C. H. K. Chemirik, « Multidimensional analysis of NDVI dynamics in response to climate and land use/land cover change in Northwest Algeria », *Journal of Hydrology and Hydromechanics*, vol. 72, nº 4, p. 399-412, déc. 2024, doi: 10.2478/johh-2024-0020.
[13] M. Grosse-Heilmann, E. Cristiano, R. Deidda, et F. Viola, « Durum wheat productivity today and tomorrow: A review of influencing factors and climate change effects », *Resources, Environment and Sustainability*, vol. 17, p. 100170, sept. 2024, doi: 10.1016/j.resenv.2024.100170.
[14] R. G. Allen, L. S. Pereira, D. Raes, et M. Smith, « Crop evapotranspiration - Guidelines for computing crop water requirements - FAO Irrigation and drainage paper 56 ».
[15] M. M. Alam *et al.*, « A review of recent advances and future prospects in calculation of reference evapotranspiration in Bangladesh using soft computing models », *Journal of Environmental Management*, vol. 351, p. 119714, févr. 2024, doi: 10.1016/j.jenvman.2023.119714.
[16] T. G. V. Niel et T. R. McVicar, « REMOTE SENSING OF RICE-BASED IRRIGATED AGRICULTURE: A REVIEW », *REMOTE SENSING*.
[17] S. Skendžić, M. Zovko, V. Lešić, I. Pajač Živković, et D. Lemić, « Detection and Evaluation of Environmental Stress in Winter Wheat Using Remote and Proximal Sensing Methods and Vegetation Indices—A Review », *Diversity*, vol. 15, nº 4, Art. nº 4, avr. 2023, doi: 10.3390/d15040481.
[18] A. T. Islam *et al.*, « Monitoring wheat area using sentinel-2 imagery and In-situ spectroradiometer data in heterogeneous field conditions », *Discov Agric*, vol. 2, nº 1, p. 52, sept. 2024, doi: 10.1007/s44279-024-00069-4.
[19] B. Duchemin *et al.*, « Monitoring wheat phenology and irrigation in Central Morocco: On the use of relationships between evapotranspiration, crops coefficients, leaf area index and remotely-sensed vegetation indices », *Agricultural Water Management*, vol. 79, nº 1, p. 1-27, janv. 2006, doi: 10.1016/j.agwat.2005.02.013.
[20] S. Er-Raki, A. Chehbouni, N. Guemouria, B. Duchemin, J. Ezzahar, et R. Hadria, « Combining FAO-56 model and ground-based remote sensing to estimate water consumptions of wheat crops in a semi-arid region », *Agricultural water management*, vol. 87, nº 1, p. 41-54, 2007.
[21] E. Farg, S. M. Arafat, M. S. Abd El-Wahed, et A. M. EL-Gindy, « Estimation of Evapotranspiration *ETc* and Crop Coefficient *Kc* of Wheat, in south Nile Delta of Egypt Using integrated FAO-56 approach and remote sensing data », *The Egyptian Journal of Remote Sensing and Space Science*, vol. 15, nº 1, p. 83-89, juin 2012, doi: 10.1016/j.ejrs.2012.02.001.
[22] G. Pakhale, P. Gupta, et J. Nale, « Crop And Irrigation Water Requirement Estimation By Remote Sensing And GIS: A Case Study Of Karnal District, Haryana, India », 2010.
[23] R. Amri, M. Zribi, Z. Lili-Chabaane, C. Szczypta, J. C. Calvet, et G. Boulet, « FAO-56 Dual Model Combined with Multi-Sensor Remote Sensing for Regional Evapotranspiration Estimations », *Remote Sensing*, vol. 6, nº 6, Art. nº 6, juin 2014, doi: 10.3390/rs6065387.
[24] M. Asadi et K. V. Kamran, « Comparison of SEBAL, METRIC, and ALARM algorithms for estimating actual evapotranspiration of wheat crop », *Theor Appl Climatol*, vol. 149, nº 1, p. 327-337, juill. 2022, doi: 10.1007/s00704-022-04026-3.
[25] X.-Y. Tong, G.-S. Xia, et X. X. Zhu, « Enabling country-scale land cover mapping with meter-resolution satellite imagery », *ISPRS Journal of Photogrammetry and Remote Sensing*, vol. 196, p. 178-196, févr. 2023, doi: 10.1016/j.isprsjprs.2022.12.011.

Table 1. The meteorological measurements for the growth phases 2017-2018. I extend my gratitude to the Sidi Bel Abbes National Meteorological Office Station for providing access to their meteorological data, which was instrumental in conducting this study.
Table 2. The predictive equations of various coefficients for stages of development.
Table 3. Correlation coefficients for different growth stages between the values of calculated and predicted K_c.
Figure 1. False colour composition images of the study area obtained by Landsat 8 satellite (5, 4, 3).
Figure 2. Normalized difference vegetation index (NDVI) for the (a) first, (b) second, and (c) third growth stages.
Figure 3. Soil-adjusted vegetation index (SAVI) for the (a) first, (b) second, and (c) third growth stages.
Figure 4. Predicted crop coefficient K_c for the (a) first, (b) second, and (c) third growth stages.
Figure 5. Predicted crop evapotranspiration ET_c for the (a) first, (b) second, and (c) third growth stages.
Figure 6. Variation of Kc, NDVI, SAVI, and predicted Kc across different growth stages.